Available online at www.sciencedirect.com

SCIENCE DIRECT®

Developmental Biology xx (2004) xxx–xxx

DEVELOPMENTAL BIOLOGY

www.elsevier.com/locate/ydbio

Beyond the *neckless* phenotype: influence of reduced retinoic acid signaling on motor neuron development in the zebrafish hindbrain

G. Begemann,* M. Marx,[1] K. Mebus, A. Meyer, and M. Bastmeyer[1]

Department of Biology, University of Konstanz, 78464 Constance, Germany

Received for publication 29 January 2004, revised 18 March 2004, accepted 29 March 2004

Abstract

Retinoic acid (RA) has been identified as a key signal involved in the posteriorization of vertebrate neural ectoderm. The main biosynthetic enzyme responsible for RA signaling in the hindbrain and spinal cord is Raldh2. However, *neckless/raldh2*-mutant (*nls*) zebrafish exhibit only mild degrees of anteriorization in the neural ectoderm, compared to full vitamin A deficiency in amniotes and the Raldh2$^{-/-}$ mouse. Here we investigated the role of RA during neuronal development in the zebrafish hindbrain and anterior spinal cord using DEAB, an inhibitor of retinaldehyde dehydrogenases. We show that the *nls* hindbrain and spinal cord are not fully devoid of RA, since blocking Raldh-mediated RA signaling leads to a more severe hindbrain phenotype than in *nls*. The anteroposterior distribution of branchiomotor neurons in the facial and more posterior nuclei depends on full RA signaling throughout early and late gastrula stages. In contrast, inhibition of RA synthesis after gastrulation reduces the number of branchiomotor neurons in the vagal nucleus, but has no effect on anteroposterior cell fates. In addition, blockage of RA-mediated signaling not only interferes with the differentiation of branchiomotor neurons and their axons in the hindbrain, but also affects the development of the posterior lateral line nerve.

Keywords: Retinaldehyde dehydrogenase; raldh2; Retinoic acid; Hindbrain patterning; Cranial motor neurons; Zebrafish

Introduction

Retinoic acid (RA) is a morphogenetically active signaling molecule with important roles in various developmental processes in vertebrates (Eichele, 1997; Morriss-Kay and Ward, 1999). The developing central nervous system (CNS) is particularly sensitive to variation in the amounts of retinoid signaling (Maden, 2002). Ectopic application of retinoic acid causes patterning defects in the hindbrain and anterior spinal cord by transforming anterior neural tissue toward a more posterior neural specification (posteriorization) (Durston et al., 1989). Excess retinoid signaling does not influence early neural induction, but it represses forebrain- and midbrain-specific gene expression domains within already induced neural tissue, while posterior markers are expanded anteriorly (Gavalas and Krumlauf, 2000).

RA is synthesized from dietary sources of vitamin A, through the oxidation to retinaldehyde by alcohol dehydrogenases and the subsequent conversion to RA by retinaldehyde dehydrogenases. In the amniote embryo, three enzymes, Raldh1 (Aldh1a1), Raldh2 (Aldh1a2) and Raldh3 (Aldh1a3), are capable of synthesizing RA. However, only Raldh2 appears to participate in the early posteriorization process of the neural tube (Niederreither et al., 2002). The effects of reduced RA signaling are mimicked by depleting the developing embryo of dietary sources of vitamin A. The ensuing developmental defects include the anteriorization of the hindbrain and are collectively known as vitamin A-deficiency (VAD) syndrome (Dickman et al., 1997; Maden et al., 1996; Morriss-Kay and Sokolova, 1996). During normal development, the vertebrate hindbrain transiently forms distinct segments called rhombomeres (r). Each rhombomere has an individual identity as exemplified by gene expression patterns and contains neurons with rhombomere-specific axon navigation behavior and neural crest cells with specific migration routes. In amniote VAD embryos, the caudal hindbrain is transformed toward more anterior fates, resulting in enlarged anterior rhombomeres and a truncation of rhombomeres posterior to r3. Through

* Corresponding author. Department of Biology, University of Konstanz, Fach M617, 78457 Constance, Germany. Fax: +49-7531-88-3018.

E-mail address: gerrit.begemann@uni-konstanz.de (G. Begemann).

[1] Present address: University of Jena, Institut für Allgemeine Zoologie und Tierphysiologie, Erbertstrasse 1, 07743 Jena, Germany.

0012-1606/$ - see front matter © 2004 Published by Elsevier Inc.
doi:10.1016/j.ydbio.2004.03.033

simultaneous application of increasing concentrations of RA to VAD rat embryos, a gradual rescue of caudal rhombomeric gene expression can be achieved (Gale et al., 1999; Maden et al., 1996).

Mutations in the zebrafish *retinaldehyde dehydrogenase 2 (raldh2)* gene, *raldh2/neckless (nls)*, have been described and recapitulate some of the phenotypes that are typical of VAD in vertebrate embryos. Both studied alleles (nls^{i26} and $nls^{no\ fin}$) exhibit defects in patterning of the caudal-most hindbrain and the spinal cord (Begemann et al., 2001; Grandel et al., 2002). The neural patterning defects are comparable to milder forms of VAD in rat embryos (White et al., 2000) and to the partial rescue of $Raldh2^{-/-}$ mice by maternal application of RA (Niederreither et al., 2000), rather than to complete elimination of RA signaling.

In contrast, the gene knockout of Raldh2 in the mouse mimics the hindbrain phenotypes associated with full VAD (Niederreither et al., 1999, 2000) and establishes Raldh2 as the main RA-producing enzyme required in the hindbrain during amniote embryonic development (Berggren et al., 1999; Niederreither et al., 1997). It is unlikely that *nls* is a hypomorphic mutation, since the non-neural developmental defects, in the *nls* branchial arch skeleton and pectoral fins, are stronger or as strong as in full VAD and $Raldh2^{-/-}$ mice, and morpholino-mediated knockdown of *raldh2* leads to exact phenocopies of *nls* (Begemann et al., 2001; Grandel et al., 2002). This raises the possibility that zebrafish may possess an additional retinaldehyde dehydrogenase, either a paralogous *raldh2* gene or another member of the Raldh-protein subfamily, that can partially compensate for the loss of RA signaling during neural patterning.

The effects of RA on patterning the neural plate have been widely studied. However, little is known about how RA signaling affects neuronal patterning and differentiation. Here we have investigated the role of RA during neuronal development in the hindbrain and anterior spinal cord using an inhibitor of retinaldehyde dehydrogenases and have characterized neuronal patterning in both *nls* and RA signaling-inhibited embryos. We asked the question, how is the differentiation and axonal projection pattern of neuronal subtypes in the hindbrain altered in RA-depleted fish? We show that the *nls* hindbrain and spinal cord are not fully devoid of RA, as blocking Raldh-mediated RA signaling leads to a more severe hindbrain phenotype than in *nls*. Inhibition of RA signaling not only interferes with the differentiation of branchiomotor neurons and their axons in the hindbrain but also affects the development of the posterior lateral line nerve.

Material and methods

Zebrafish husbandry

London wild type and WIK strains of zebrafish were reared and staged at 28.5°C according to Kimmel et al. (1995). The mutant phenotypes of both *raldh2* alleles, nls^{i26} (Begemann et al., 2001) and $nls^{no\ fin}$ (Grandel et al., 2002), cannot be distinguished from each other, and experiments were performed with both alleles. Transgenic zebrafish expressing GFP under the control of the *islet-1* gene regulatory elements were kindly provided by S.I. Higashijima (Higashijima et al., 2000).

In situ hybridisation

Whole mount in situ hybridisation was performed as previously described (Begemann et al., 2001), using the following probes: *hoxb4a* (Prince et al., 1998), *isl-1* (Inoue et al., 1994), *krox-20* (*egr2b*; www.zfin.org) (Oxtoby and Jowett, 1993), *pax2a* (Krauss et al., 1992), *raldh2* (Begemann et al., 2001), *val* (Moens et al., 1998).

Retinoic acid and DEAB treatments

Batches of embryos from wild type or *nls* heterozygous parents were incubated in the dark from late blastula stage onwards in varying dilutions (in embryo medium) of a 10^{-4} M all-trans RA (Sigma)/10% ethanol solution (from a 10^{-2} M stock solution in DMSO). DEAB (4-diethylaminobenzaldehyde; Fluka) was applied in the dark, in concentrations of 10^{-5} M and 2×10^{-5} M in embryo medium from a 10^{-2} M stock in DMSO. BMS493 was diluted to 10^{-5} and 10^{-6} M from a 10^{-2} M stock solution in ethanol. As controls, sibling embryos were treated with equivalent concentrations of ethanol/DMSO or DMSO alone.

Antibody staining and analysis

Zebrafish embryos were processed for whole-mount immunohistochemistry as previously described (Weiland et al., 1997). Briefly, embryos were fixed for 4 h at 4°C in 4% paraformaldehyde in 1× fixation buffer (Westerfield, 1995) and permeabilized by exposure to acetone (−20°C for 2–3 min). After incubation in blocking buffer (PBS with 1% BSA, 1% DMSO) for 1 h at 37°C, they were exposed to primary antibodies overnight at 4°C. To visualize zebrafish axons the following antibodies were used: a monoclonal antibody against zebrafish L1 (zL1, Mab E17, 25 μg/ml; Weiland et al., 1997), a monoclonal IgG-antibody against the polysialated form of NCAM (PSA, Mab 735, 25 μg/ml; kindly provided by R. Gerardy-Schahn), a monoclonal IgM-antibody against PSA (Mab 12E3, 20 μg/ml; Marx et al., 2001), and a polyclonal serum against zebrafish TAG-1 (zTAG-1; Lang et al., 2001; Ott et al., 2001). Embryos were rinsed in blocking buffer and incubated with the following secondary antibodies: Alexa-488-coupled goat anti-rabbit (2 μg/ml; Molecular Probes), Alexa-488-coupled goat anti-mouse (2 μg/ml; Molecular Probes), cyanin-3-coupled donkey anti-mouse IgG (H+L) (2 μg/ml; Dianova), or cyanin-3-coupled goat anti-mouse IgM, μ-chain specific (2 μg/ml, Dianova), for 2 h at 37°C. For microscopy, yolk sacs were

removed and embryos were embedded in Mowiol (containing n-propylgallate as an antifading agent) between two coverslips. GFP-fluorescence was assayed immediately following fixation. Stained embryos were analyzed with a confocal microscope (LSM 510, Zeiss, Jena, Germany) equipped with high aperture lenses and the appropriate lasers. Serial optical sections were flattened into projections. All images were further processed with Adobe Photoshop 6.0 software.

Results

Inhibitors of RA signaling phenocopy nls/raldh2 to various amounts

Compared to the inactivation of *Raldh2* in the mouse, *nls/raldh2* mutant embryos resemble a state of intermediate vitamin A deficiency (Begemann et al., 2001; Grandel et al., 2002). However, the effects of targeted knockdown of *raldh2* mRNA and the molecular nature of both alleles of *raldh2* in zebrafish suggests that they are complete loss-of-function mutations. Therefore, it is conceivable that *nls* mutants retain low levels of RA activity, which may be provided maternally or from a yet unidentified enzymatic activity other than *nls/raldh2*. To test this possibility, zebrafish embryos were treated with two different chemicals which interfere with RA signaling. We used either BMS493, a pan-retinoic acid receptor antagonist, or diethylaminobenzaldehyde (DEAB), a competitive, reversible inhibitor of retinaldehyde dehydrogenases (Perz-Edwards et al., 2001; Russo et al., 1988).

Wild type embryos were treated with BMS493 or DEAB starting at 5-h post-fertilization (hpf) and investigated at 40 hpf. At the morphological level, embryos treated with either inhibitor exhibit most of the developmental defects specific to *nls* embryos. These include a reduction of head mesoderm along the anteroposterior (AP) axis, resulting in close apposition of otic vesicle and trunk somites, and a shortening of the hindbrain, resulting in a pronounced kink at the hindbrain–spinal cord junction (Figs. 1A–D). Furthermore, like in *nls* mutants, pectoral fin buds fail to form and cardiac edema develop after 48 hpf (not shown).

We next assayed segmental patterning in the hindbrain. In the wild type, *krox-20* is expressed in a segment-specific pattern in r3 and r5, while *hoxb4a* is expressed in r7 and extends posteriorly in the spinal cord (Fig. 2A). In *nls*, expression of *krox-20* in both rhombomeres is slightly expanded and expression of *hoxb4a* is present at 20 h post fertilization (hpf), suggesting that rhombomeres are mildly posteriorized (Fig. 2B). When treated with 10^{-5} M BMS493, rhombomeric gene expression is similar to and not significantly more severe than *nls* (Fig. 2C) (Grandel et al., 2002). When treated with DEAB, expression of *krox-20* is greatly reduced in r5 and remains only in its anterior most part; the concomitant loss of *hoxb4a* expression suggests that rhombomere boundaries posterior to r5 do not form (Fig. 2D). As expected, application of

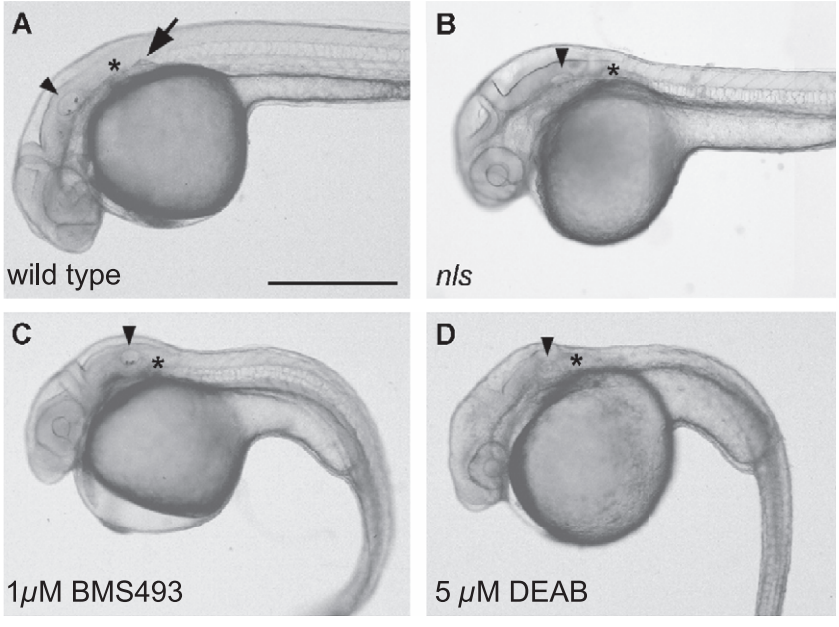

Fig. 1. Developmental defects in live embryos at 40 hpf when retinoic acid signaling is impaired. (A) Wild type embryos are characterized by a large distance between otic vesicle (arrowhead) and first somite (asterisk); the pectoral fin buds are well developed (arrow). (B) In *nls* mutant embryos, the head is characteristically foreshortened, the distance between otic vesicle and first somite is reduced, and pectoral fin buds fail to develop. (C) Inactivation of RA signaling with the pan-RA receptor antagonist BMS493 exhibits very similar phenotypes in the hindbrain and pectoral fin buds. (D) Embryos exposed to DEAB from 50% epiboly onwards display a *nls*-like phenotype; the distance between otic vesicle and first somite is dramatically reduced; pectoral fin buds are missing. Lateral views; anterior to the left. Scale bar, 500 μm.

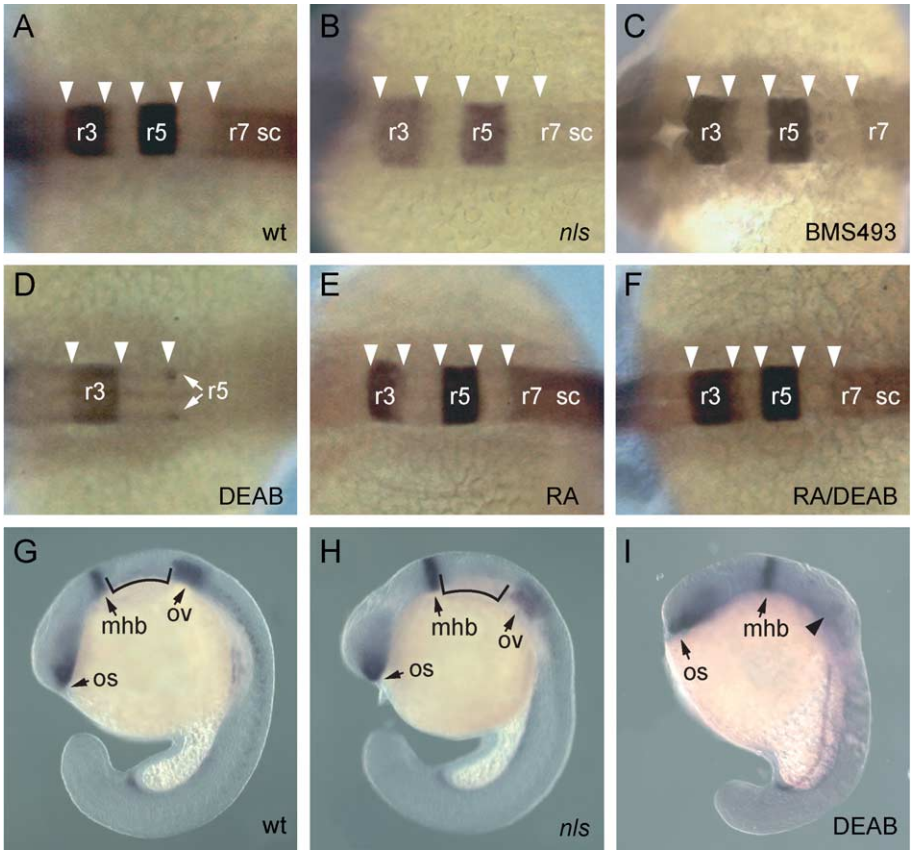

Fig. 2. Hindbrain patterning defects in response to alterations in retinoic acid signaling. Expression of *krox-20* in rhombomeres (r) 3 and r5, and *hoxb4a* in the neural tube, posterior to the r6/r7 boundary, in 20 hpf wild type embryos (A); posterior expansion of r3-5 in *nls* mutant embryos, *hoxb4a* expression is present, but often weaker (B); 10 μM of the pan-RAR antagonist BMS493 phenocopies posterior expansion of r3-5 rhombomere boundaries in *nls*; *hoxb4a* expression is present, but extends less posteriorly than in wt or *nls* (not shown) (C). Five-micromolar DEAB anteriorizes the hindbrain further than observed in *nls* or BMS493-treated embryos (note expansion of r3 and r4), markers of pre-rhombomeric fates posterior to the r4/r5 boundary are reduced (arrows) (D); treatment with 10 nM RA results in variable levels of posteriorization, as indicated by the reduction of r3; at higher doses (not shown), r3 expression is undetectable (E); simultaneous treatment with 10 nM RA and 5 μM DEAB rescues normal hindbrain development, and restores *hoxb4a* expression in the spinal cord (F). Expression of *pax2a* delineates the increase in distance (indicated by bracket of identical length in G, H) between the midbrain–hindbrain boundary (mhb) and the otic vesicle (ov) in wt (G) and *nls* (H) embryos at 20 hpf; in DEAB-treated embryos (I) expression in the otic vesicles is reduced, sometimes to complete absence, while the mhb appears unaffected. Arrowheads denote visible rhombomere boundaries. Abbreviations: os: optic stalk, sc: spinal cord; dorsal (A–F) and lateral (G–I) views, anterior to the left.

RA alone leads to an anteriorization of the hindbrain, greatly reducing r3 and expanding r5 anteriorly (Fig. 2E) (Hill et al., 1995; Holder and Hill, 1991). Most importantly, the patterning defects in DEAB-treated embryos can be rescued through simultaneous application of RA to revert to an almost wild type appearance (Fig. 2F), suggesting that the anteriorizing effect of DEAB can be attributed to a reduction in RA signaling.

To compare the AP-extension of the hindbrain anterior to r3, we used the expression of *pax2a*, a marker for the ventral diencephalon, the midbrain–hindbrain boundary (mhb), and the otic placode, as well as *valentino* (*val*) to mark r5 and r6 (Fig. 2G). In *nls*, the mhb is located slightly more posterior than in wild type; similarly, the otic vesicles are shifted posteriorly, probably due to the caudal expansion of r5 fates, as witnessed by a small widening of *val* expression in the AP direction (Fig. 2H). As in *nls*, DEAB-treated embryos also exhibit a small shift of the mhb posteriorly, while expression of *pax2a* in the otic vesicle is variably reduced (Fig. 2I).

These results suggest that the teratogenic effects of DEAB in the developing neural tube are due to inhibition of retinaldehyde dehydrogenase-mediated RA synthesis. The phenotypes are comparable to the inactivation of RALDH2 in amniotes and reveal a state of RA deficiency in the zebrafish beyond that observed in *nls*.

Development of cranial motor neurons in the absence of RA

Each hindbrain rhombomere is unique and characterized by differences in size, number, and projection patterns of specific neuronal populations. To analyze the effects of reduced RA signaling on the differentiation of branchiomotor neurons in the hindbrain, we used a transgenic line expressing green fluorescent protein (GFP) under the control of the *islet-1* (*isl-1*) promoter (Higashijima et al., 2000).

In this line, cell bodies and axons of motor neurons in the hindbrain and spinal cord can be visualized throughout development (Fig. 3A). To relate changes in the anteroposterior positions of branchiomotor nuclei nVII–nX to earlier patterning defects, we measured their location in relation to the trigeminal nucleus (nVa), whose position was invariable with respect to the eyes in these experiments. Embryos were treated continuously up to 39 hpf with two concentrations of inhibitor, commencing at varying time points of embryonic development.

Inhibition of RA signaling between 11 and 39 hpf (prim-28; (Kimmel et al., 1995) does not influence the anteroposterior position of branchiomotor neurons (Figs. 3B, E). In all cases, we neither observed a reduction in the AP extent of the vagal (nX) field, nor were developmental or patterning defects apparent in more anterior regions. However, we consistently observed a reduction in the number of branchiomotor neurons in the vagal nucleus (nX) to approximately 25–50% of the numbers found in wild type embryos. These data suggest, that after the onset of somitogenesis, RA influences neurogenesis or differentiation of the vagal motor nerves, whereas AP patterning of the motor region is not affected by DEAB treatments after gastrulation.

When RA signaling was inhibited starting during mid-gastrulation, from 8 hpf (75% epiboly) onwards, the AP extent of branchiomotor neurons in the vagal lobes is reduced in comparison with the wild type, as is the number of neurons in branchiomotor nuclei (Figs. 3C, F). No aberrant neural development anterior to nX was observed. DEAB treatment from 6 hpf (shield stage) onwards reduces the number of GFP-positive cell bodies in the vagal nucleus (nX), both at 28 hpf (not shown) and 39 hpf (Figs. 3D, G). In addition, the AP extent of the vagal (nX) nucleus is considerably reduced (Figs. 3D, G). The more anteriorly positioned branchiomotor nucleus of the facial nerve (nVII) also develops aberrantly. No defects in development of branchiomotor neurons were evident anterior to nVII. The nucleus of the glossopharyngeal nerve (IX), situated between nVII and nX, consists only of a few GFP-positive neurons and therefore could not be assayed in this study. We conclude that the number of branchiomotor neurons in the vagal nucleus, as well as the anteroposterior distribution of

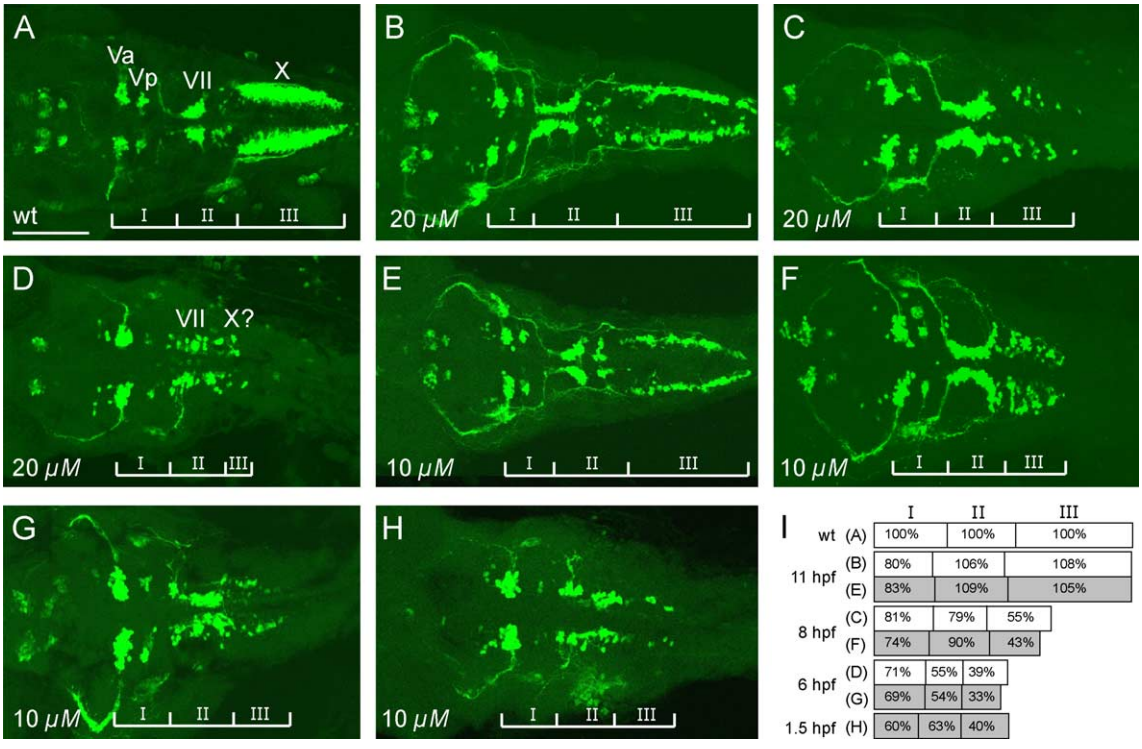

Fig. 3. Morphological changes in cranial motor neurons upon RA signaling inhibition. (A) Dorsal view of cranial motor neurons expressing Isl1-GFP at 39 hpf in a wild type embryo. Brackets mark division into three anteroposterior areas, comprising trigeminal branchiomotor (Va, Vp; area I), facial (VII; area II) and vagal nuclei (X; area III). (B–D) Inhibitor treatment (20 μM DEAB) commencing at 11 hpf (B), 8 hpf (C) and 6 hpf (D) results in increased shortening of all anteroposterior areas of the hindbrain; (B) the numbers of vagal nuclei are strongly reduced, when inhibition of RA signaling commences during early somitogenesis (11 hpf); the posterior extent of the vagal area is unaffected; (C) treatment at mid-gastrulation (8 hpf onwards) reduces vagal nuclei in both posterior extent and number; facial nuclei are clearly separated; (D) when inhibition commences at shield stage (6 hpf), both facial and vagal nuclei are reduced in number and develop near, such that the border between these cell types cannot be distinguished accurately by position. (E–H) 10 μM DEAB treatment commencing at 11 hpf (E), 8 hpf (F), 6 hpf (G), and 1.5 hpf (H) results in comparable reductions; exposure to 10 μM DEAB from the 16-cell stage onwards (H) does not exacerbate either the anteroposterior patterning defects nor reductions in cell number observed in (D) and (G). (I) Graphical representation of alterations to branchiomotor neuron patterning upon RA signaling inhibition (based on 20 embryos each; Table 1); the average anteroposterior length of individual sectors is compared to untreated embryos and indicated as percent (%); grey bars indicate 10 μM DEAB concentration. (A–H) Dorsal views, anterior is to the left. Scale bar: 100 μm.

these neurons, depends on full RA signaling throughout early and late gastrula stages. The development of more anterior branchiomotor neurons, such as the facial nucleus (nVII), is insensitive to DEAB treatment at 11 hpf, but is affected by earlier treatments (see below).

It is conceivable that contribution of Raldh2 mRNA or protein from the maternal genome may retain residual signaling activity before shield stage. Therefore, we applied DEAB at 1.5 hpf (16-cell stage). At concentrations of 5 μM (not shown) and 10 μM (Fig. 3H), these phenotypes are not significantly stronger than those of embryos treated at 6 hpf (Figs. 3H, I; Table 1). Embryos incubated similarly in 20 μM DEAB develop aberrantly and die before 39 hpf, indicating that 10 μM treatments achieve a maximum level of inhibition. These results suggest that RA signaling before 6 hpf has little or no influence on the patterning of developing cranial motor neurons.

To determine the consequences of reduced RA signaling in *nls*, we detected *isl-1* expression in *nls* and in embryos treated with 10 μM DEAB. Changes in motor neuron patterning observed with *isl-1* mirror those seen in the Isl1-GFP line (Fig. 4). Cranial motor neurons in *nls* resemble a state of RA-signaling that is intermediate between the phenotypes resulting from DEAB treatment commencing during (6 hpf) and after (11 hpf) gastrulation (Fig. 4C). The relatively mild reduction in AP extent of the vagal nucleus confirms that Raldh2 acts during gastrulation stages and implies the presence of additional sources of RA during gastrulation.

Development of cranial nerve projections in the absence of RA

To analyze the axonal projection pattern of branchiomotor neurons after inhibition of RA-mediated AP signaling in more detail, we labeled embryos with antibodies against zebrafish L1 (zL1) and polysialic acid (PSA). zL1 is expressed in a spatiotemporal pattern on all axons during development and therefore serves as a pan-axonal marker (Weiland et al., 1997). Antibodies against PSA, a sugar epitope on the neural cell adhesion molecule, selectively label motor axons in cranial nerves V, VII, IX, and X (Marx et al., 2001).

Table 1
Temporal requirement of RA signaling for motor neuron patterning

Concentration of inhibitor (μM)	Commencement of inhibition (hpf)	Length of all sectors I + II + III (μm)	Length of each area[a] (μm)		
			I	II	III
0 (controls)	0	380	108	100	173
10	1,5	191	65	63	70
10	6	184	76	55	66
10	8	235	87	79	95
10	11	378	86	106	186
20	6	191	75	54	57
20	8	238	80	90	74
20	11	378	89	109	180

[a] The hindbrain was divided into three areas, roughly corresponding to the position of the trigeminal nuclei and exit points of the facial nerves (nV-nVII; sector I), posterior facial and glossopharyngeal nuclei (nVII-nIX; sector II), and vagal nuclei (nX, sector III). Lengths were averaged for the sample size (n = 20) and were compared between untreated controls and RA signaling-inhibited larvae at 39 hpf.

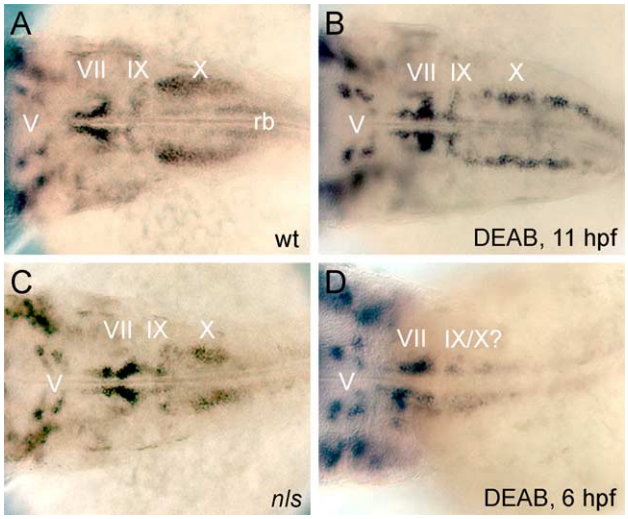

Fig. 4. *islet-1* expression pattern in cranial motor neurons upon RA signaling inhibition. (A–D) Dorsal views of *islet-1* expression in 39 hpf embryos. (A) In wild type, *islet-1* mRNA is expressed in trigeminal (V), facial (VII), glossopharyngeal (IX) and vagal (X) motor neurons, and in Rohon-Beard neurons (rb) in the spinal cord. (B) *islet-1* expression in wild type embryos treated with 10 μM DEAB from 11 to 39 hpf. (C) *islet-1* expression in *nls* embryos. (D) *islet-1* expression in wild type embryos treated with 10 μM DEAB from 6 to 39 hpf; posterior cranial motor neurons cannot be unambiguously identified.

Ventral views of double labeled control embryos at 48 hpf reveal the locations of branchiomotor nuclei in the hindbrain and the typical pathways of cranial nerves in the peripheral nervous system (PNS) (Fig. 5A). The original stacks of the confocal images were used to generate a graphical reconstruction for better discrimination of the various branches (Fig. 5B). In *nls* mutants, axons innervating the mandibular (V) and hyoid (VII) arch are present, but their normal projection pattern is altered to variable amounts (Figs. 5C, D). The medial projecting branch of the trigeminal nerve (Va) is missing in 50% of *nls* embryos, whereas the two anterior projecting branches (Vb, Vc) are not affected (Fig. 5D). In DEAB-treated embryos, the nuclear region of nVII is enlarged (measuring an averaged 29 μm, against 20 μm in *nls*) and appears to be located more dorsally within the hindbrain. In addition, one facial nerve branch (VIIa) is missing in about 80% of the investigated embryos (N = 40), while the other facial nerve branches (VIIb, VIIc) appear normal. The nuclei of cranial nerves IX and X are reduced in size and only a few, short PSA-positive vagal and glossopharyngeal axons exit the hindbrain (Figs. 5C, D).

DEAB-treated embryos exhibit more severe defects (Figs. 5E, F). In all investigated embryos (N = 50), the vagal nucleus (nX) is reduced to variable amounts and vagal axons are missing entirely. Facial and trigeminal nuclei are

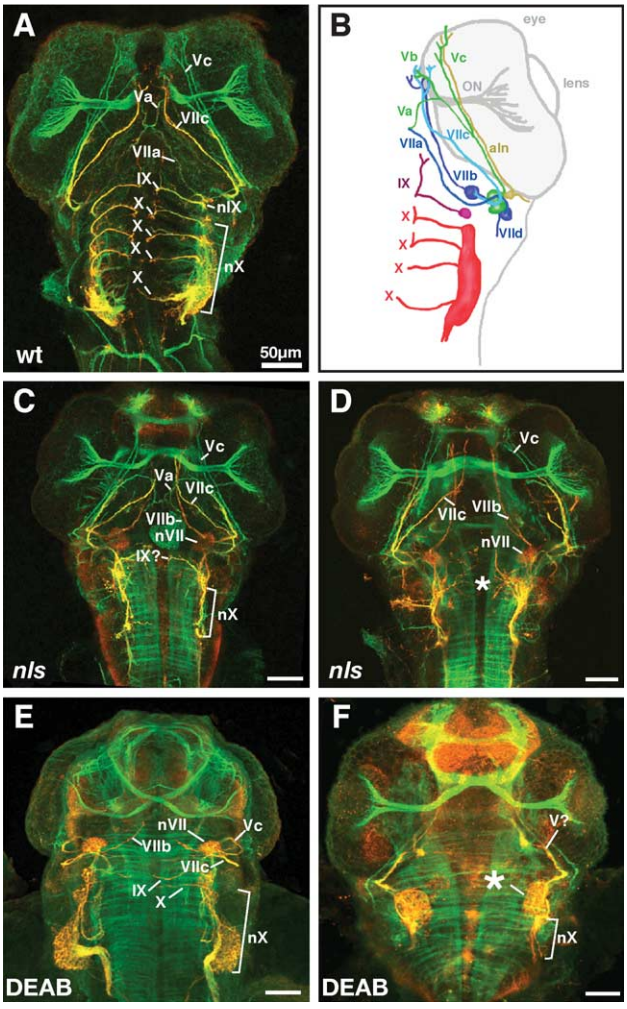

Fig. 5. Projection pattern of cranial nerves in *neckless* and DEAB-treated embryos. Projections of confocal images of 48 hpf embryo wholemounts stained with antibodies against zL1 (green) and PSA (red). (A) In control embryos, zL1 is expressed on all axons, whereas PSA selectively labels motor axons in cranial nerves V, VII, IX, and X. (B) Schematic drawing derived from the original stack shown in A, illustrating the nuclei and pathways of cranial nerves in color coding. In *nls* mutants (C, D), the nucleus of cranial nerve X (nX) is reduced in size and only a few, short PSA-positive vagal axons (X) leave the hindbrain. The facial nucleus (nVII) is enlarged and one facial nerve branch (VIIa) is missing. The other facial nerve branches (VIIb, VIIc) appear normal. The medial-projecting branch of the trigeminal nerve (Va) is missing in 50% of *nls* embryos (D), whereas the two anterior projecting branches (Vb, Vc) are not affected. In DEAB-treated embryos (E, F), the vagal nucleus (nX) is reduced to variable amounts and vagal axons (X) are either missing (F) or rudimentary present (E). The facial nucleus (nVII) is either enlarged in size (E) or fused with other PSA-positive neurons to a single structure (asterisk in F). Ventral (A–D) and dorsal (E, F) views, anterior is to the top. Scale bars: 50 µm.

fused and no longer distinguishable as single nuclei, and the glossopharyngeal nerve is always absent. Consistent with our observed effects on pre-rhombomeric gene expression, the stronger phenotypes in all posterior motor domains suggest that DEAB reduces RA signaling more severely than in *nls*. Interestingly, we noted that the staining of PSA appears to be more intense in *nls* and DEAB-treated embryos as compared to controls. This might indicate a regulatory function of retinoic acid on the amount of PSA expression during development.

To analyze whether other axon projection patterns are also affected by inhibition of RA signaling, we labeled embryos with an antibody against TAG-1. In the zebrafish PNS, TAG-1 is expressed by cell bodies and axons of motor neurons in the spinal cord, dorsal root ganglion cell bodies and their axons, and the lateral line nerves (Ott et al., 2001). In control embryos, motor nerves from the first three spinal cord segments first project distally onto the yolk and then turn rostral (Fig. 6A). Although these motor nerves are present in *nls* mutants and their growth pattern is not affected, they are shorter (Fig. 6B). Following DEAB-treatment, the motor nerve from the first segment is absent in about 10% of the embryos (Fig. 6C). In addition, the growth pattern of the first three motor nerves on the yolk is altered. Branching of these nerves is reduced and instead of turning rostral the nerves project further distally. Growth patterns of motor axons caudal to the third spinal segment are not affected in *nls* mutants or after DEAB treatment (not shown). This suggests that RA signaling is not involved in motor neuron induction in the spinal cord, but is required for the establishment of growth patterns of the first three spinal motor nerves.

Sensitivity of lateral line nerve projections to RA signaling

We also noted that inhibition of RA signaling interferes with the development of the lateral line nerves. At 48 hpf, the anterior and posterior lateral line nerves are well developed in control embryos (Figs. 7A, B) and axons of the posterior nerve have reached the last myotome (not shown). In *nls* mutants, the anterior lateral line nerve is present and its growth pattern is indistinguishable from that seen in controls. However, the posterior lateral line nerve is always markedly reduced in diameter (Fig. 7C) and fails to grow beyond the first myotome in about 30% of mutants (Fig. 7D). In addition, the ganglion of the posterior lateral line nerve is always reduced in size (Figs. 7C, D). In DEAB-treated embryos, the anterior lateral line nerve is again not affected (Fig. 7E). In contrast, the posterior lateral line nerve develops only rudimentary stumps in all embryos (Figs. 7E, F). The ganglion of the posterior lateral line nerve is particularly reduced in size and often fused with remnants of other sensory ganglia (Figs. 7E, F). These findings further point toward a role of RA-mediated AP signaling in the development of the posterior lateral line system.

Discussion

Raldh2 and additional sources of RA contribute to neural AP patterning

We have studied the effects of inhibiting RA signaling on hindbrain segmentation and subsequent neuronal patterning

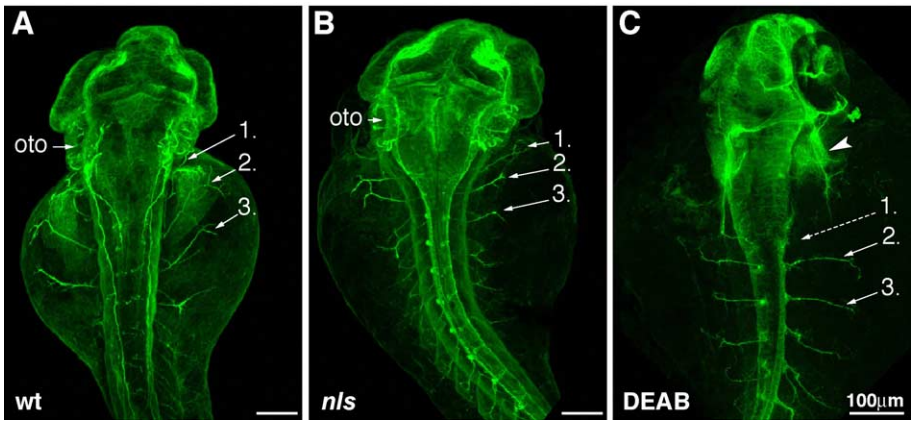

Fig. 6. Projection pattern of motor neurons in *neckless* and DEAB-treated embryos. Projections of confocal images of 48 hpf embryo wholemounts stained with an antiserum against zfTag-1, which is expressed by motor axons in the spinal cord. In control embryos, motor nerves from the first three spinal cord segments first project distally onto the yolk and then turn rostral (A, 1–3). In *nls* these three motor nerves are present, but they appear to be shorter (B, 1–3). After DEAB-treatment, the motor nerve from the first segment is missing in about 10% of the embryos (C, dotted line) and the growth pattern of the first three motor nerves on the yolk is less branched and directed distally. Dorsal views, anterior is to the top. Oto: otholith. Scale bars: 100 µm.

in the developing zebrafish neural tube. When compared to VAD in birds and rats (Gale et al., 1999; Maden et al., 1996; White et al., 2000), interference with RA receptor activities in frog and mouse (Dupé et al., 1999; van der Wees et al., 1998; Wendling et al., 2001), and the Raldh2$^{-/-}$ mouse (Niederreither et al., 2000), the segmental organization and gene expression of the RA-deficient hindbrain in *nls* zebrafish resembles a state of reduced, but not completely inhibited, RA signaling activity.

BMS493 inhibits the activation of all three RA-receptor (RAR) subforms in amniotes (Dupé and Lumsden, 2001; Wendling et al., 2000) and is thought to act by reinforcing co-repressor binding to RAR; moreover, antagonist binding enhances the silencing effect of unliganded retinoid receptor complexes (RAR/RXR) bound to retinoic acid response elements (Germain et al., 2002). Application of BMS493 to zebrafish embryos leads to almost exact phenocopies of *nls* in the posterior hindbrain (Fig. 2C) (Grandel et al., 2002). Although this reinforces the notion that *nls* mutants are devoid of RA signaling from *nls/raldh2*, it is possible that BMS493 may not efficiently inhibit all RAR-mediated signaling in zebrafish. Thus, alternative agents, which inhibit RA signaling, may be required to investigate the full extent of RA function during neural patterning in zebrafish. Citral, a competitive inhibitor of the aldehyde dehydrogenase-mediated oxidation of retinol and retinal to RA (Chen et al., 1995; Connor and Smit, 1987; Kikonyogo et al., 1999) and disulfiram, which inhibits the activity of aldehyde dehydrogenase class 1 enzymes (Vallari and Pietruszko, 1982; Veverka et al., 1997), are likely to display a comparatively wide substrate specificity. Therefore, we applied DEAB to block RA synthesis. DEAB is a compet-

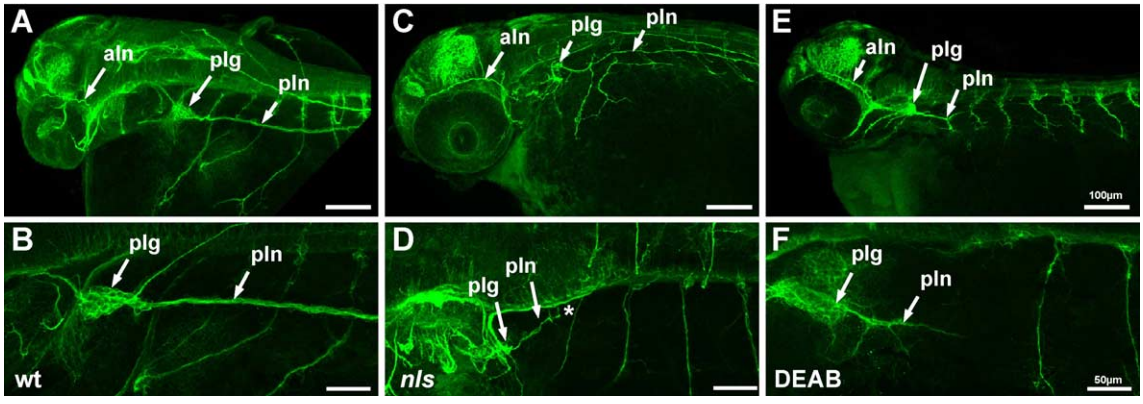

Fig. 7. The posterior lateral line nerve is affected in *neckless* and in DEAB-treated embryos. Projections of confocal images of 48 hpf embryo wholemounts (A, C, E: overviews; B, D, F: higher magnifications of the posterior lateral line system in different embryos) stained with an antiserum against zTAG-1, which is expressed by ganglia and axons of the lateral line nerves. In control embryos (A, B), the anterior (aln) and posterior (pln) lateral line nerves are well developed. In *nls* mutants (C, D), the aln is present, however, the pln is always remarkably reduced in diameter (C) and often fails to grow beyond the first myotome (D, asterisk). In addition, the ganglion of the posterior lateral line nerve (plg) is always reduced in size (C, D). In DEAB-treated embryos (E, F), the aln is not affected (E) but the pln develops only rudimentary stumps (E, F). The plg is remarkably reduced in size and often fused with remnants of other sensory ganglia (E, F). Lateral views, anterior is to the left. Scale bars: 100 µm (A, C, E) and 50 µm (B, D, F).

itive, reversible inhibitor antagonist that acts as substrate of retinaldehyde dehydrogenases, but not on Aldh2 or Aldh3 (Russo et al., 1988, 2002). Furthermore, inhibition of RA synthesis with DEAB in a zebrafish transgenic reporter line (RGYn2), in which yellow fluorescent protein is under the control of RA-response elements, leads to loss of reporter activation in tissues that exhibit mutant phenotypes in *nls* (Perz-Edwards et al., 2001), suggesting that DEAB strongly inhibits Raldh2 activity in embryonic zebrafish.

Our analysis shows that DEAB treatment affects AP patterning of the neural tube in a similar fashion as seen in full VAD in amniotes. The neural tube is strongly anteriorized, and the expansion of the hindbrain posterior to r5 is prevented. Some of the other developmental defects in *nls*, including absence of forelimbs and reduction of branchial arches, are stronger or as strong as in full VAD or in the *Raldh2*$^{-/-}$ mouse. It is therefore likely that *nls* embryos retain levels of RA signaling, particularly in the posterior neural tube, which suffice for proper neural patterning. One formal possibility for this could be a maternal supply of RA itself in *nls* embryos. Alternatively, the presence of other retinaldehyde dehydrogenases may compensate for a complete loss of RA signaling. A survey of all zebrafish nucleotide entries in GenBank (540 000 sequences; October 2003) for the three members of the retinaldehyde dehydrogenase subfamily (Aldh1a1, -a2, -a3) currently identifies only Raldh2 (Aldh1a2). Our attempts to clone the remaining Raldhs by RT-PCR using degenerate primers so far were unsuccessful and genomic scaffolds of the zebrafish genome presently contain parts of the *raldh2* locus only (Ensembl contig: ctg12959). Nevertheless, since the puffer fish genome appears to contain orthologs of all three Raldhs (encoded on scaffolds FM_M001420, FM_M000233, FM_M004033), the identification of orthologs of the remaining enzymes in zebrafish can be expected soon.

Interestingly, in Raldh2$^{-/-}$ mutant mouse embryos, an RA-producing activity in the ventral hindbrain during the establishment of rhombomeric boundaries has been inferred from the activation of a RA reporter in conditionally rescued mutants (Mic et al., 2002; Niederreither et al., 2002). None of the known Raldhs are expressed in this region, suggesting the existence of an as yet uncharacterized enzymatic activity that provides RA to the posterior hindbrain and anterior spinal cord. The presence of almost normal hindbrain segmentation in *nls* mutant zebrafish suggests that such an activity is present in zebrafish, where it acts in parallel to Raldh2 and partially complements its function. In contrast to the mouse, this implies that at least two independent RA-producing activities have to be involved in neural patterning along the anteroposterior axis. It will therefore be interesting to identify additional sources of RA and then to investigate whether in fish there is partial redundancy between two synthetic pathways and whether the synthetic proteins are expressed in non-overlapping domains.

Formation of cranial motor neurons in anteriorized neural tubes

A decrease in the level of RA signaling anteriorizes the neural plate, such that rhombomere boundaries are shifted posteriorly, concomitant with a loss of rhombomeric gene expression in the more posterior regions of the hindbrain. A detailed description of the development of cranial motor nuclei under reduced RA signaling has been missing so far. We have therefore analyzed the relative positions of cranial motor neuron cell bodies and used them as landmarks to determine the effects on AP patterning in DEAB-treated embryos. Motor neuron cell bodies were visualized in a transgenic zebrafish line expressing GFP under the control of the *islet-1* promoter. To study the projection patterns of specific axonal populations, we used several antibodies against axonal cell surface components. These antibodies either served as pan-axonal markers (zL1) or selectively label well-defined subpopulations of axons including motor axons (PSA) and the lateral line nerves (TAG-1).

By analyzing the effects of commencing inhibition of RA signaling at various time points, we find that inhibition of RA synthesis after 11 hpf leads to a substantial reduction in the number of vagal (X) neurons. Thus, after the end of gastrulation AP patterning of hindbrain motor neurons is largely independent of RA signaling and implies a further role for RA in promoting proliferation or differentiation of cranial motor neurons.

As expected from the early changes in AP patterning derived from gene expression studies (Begemann et al., 2001; Grandel et al., 2002), a reduction of levels of RA synthesis during gastrulation shortens the posterior extent of the hindbrain, characterized by vagal nuclei and their axons, in a time- and concentration-dependent manner. Alterations in RA signaling during gastrula stages, when hindbrain rhombomeres are patterned, have much more profound effects on the position of posterior rhombomere boundaries than on anterior ones. Consequently, we find that disrupting RA signaling during this period largely affects the development of posterior cranial nerves (VII and X). AP patterning of motor neurons in the midbrain (III) and anterior hindbrain (V) is not altered. Because the nuclei of cranial nerve V originate in rhombomeres r2 and r3, we conclude that RA does not influence neuronal development anterior to r3.

Interestingly, when RA signaling is decreased, the anterior-most area of the hindbrain, which in our analysis includes the branchiomotor nuclei of the trigeminal (V) and facial (VII) nerves, is reduced in length (Fig. 3I). This seems surprising, as segmental gene expression domains that precede this area at neurula stages are expanded posteriorly. Even though inhibition of RA before the tailbud stage posteriorizes the neural tube, resulting in enlarged rhombomeres that contain more cells of the same segmental fate, the corresponding areas at 39 hpf are shorter than in

wild type embryos. Moreover, we find that brains of *nls* and DEAB-treated embryos, compared to wild type, are consistently enlarged along the medio-lateral axis (Figs. 3, 4). Together, this indicates that RA signaling appears to be involved in the regulation of cell movements that underlie morphogenesis of the larval brain. In support of this, BMS493 or DEAB treatments after the tailbud stage (Grandel et al., 2002, and not shown) do not posteriorize the neural tube, yet territories of anterior rhombomeres are still shortened when antagonist is applied between 11 and 39 hpf (Figs. 3B, E, I).

Why do posterior cranial motor neurons develop at all in RA-deficient brains?

Probably most surprisingly, our data suggest that branchiomotor neurons in the posterior hindbrain (VII, X) develop to some extent, despite the absence of rhombomeric patterning posterior to r5. Although in zebrafish the facial (VII) neurons are in r6 and r7, the developmental expression of neuronal markers suggests that facial neurons originate in an area encompassing r4 to r6 early in development and finally come to be positioned in r6 and r7 (summarized in Chandrasekhar et al., 1997). Similarly, a caudally directed migration of nVII neurons is thought to establish the adult pattern of branchiomotor nuclei in sharks and in many other vertebrates (Chandrasekhar et al., 1997; Gilland and Baker, 1993, and references therein). The presence of facial nuclei even in the most rigorously RA signaling inhibited hindbrains could therefore be a result of their caudal migration into an area mispatterned through anteriorization. Our results imply that such a caudal migration is independent of RA signaling. This explanation may similarly account for the presence of nVII cranial ganglia in Raldh2$^{-/-}$ mice. In the mouse, nVII nuclei are in r4 and r5, with a few in r6 (Carpenter et al., 1993). Their presence in Raldh2$^{-/-}$ knockouts, where segmentation is aberrant in r4 and is undetectable in an area spanning r5 to r8 (Niederreither et al., 2000), was therefore unexpected. Neuronal migration of nVII neurons caudally from r4 into r5 and r6 in the mouse has been suggested (Fritzsch, 1996; Goddard et al., 1996; Studer et al., 1996), however, early migration of nVII neurons in either fish or amniotes awaits direct demonstration.

Vagal (X) neurons are most severely affected in RA signaling deficient embryos. The branchiomotor nuclei of the vagal nerves are in the caudal hindbrain, posterior to r7, an area that is differently organized than the remaining hindbrain and superficially unsegmented. Even at the highest antagonist concentrations, applied from the 16-cell stage onwards, a few vagal nerves always appear to develop (Figs. 3H, 4F). Their origin is unknown and they may remain either due to inefficient RA signaling inhibition, or pathways other than RA signaling may be involved in patterning the hindbrain–spinal cord junction.

Acknowledgments

We thank Rita Hellmann, Torsten Ruest and Birte Kalveram for technical assistance, and Bristol Myers Sqibb for the kind gift of BMS493. This work was funded by grants from the Deutsche Forschungsgemeinschaft to G.B. (BE 1902/3-1) and to M.B. (BA 1034/13-1).

References

Begemann, G., Schilling, T.F., Rauch, G.J., Geisler, R., Ingham, P.W., 2001. The zebrafish *neckless* mutation reveals a requirement for *raldh2* in mesodermal signals that pattern the hindbrain. Development 128, 3081–3094.

Berggren, K., McCaffery, P., Dräger, U., Forehand, C.J., 1999. Differential distribution of retinoic acid synthesis in the chicken embryo as determined by immunolocalization of the retinoic acid synthetic enzyme, RALDH-2. Dev. Biol. 210, 288–304.

Carpenter, E.M., Goddard, J.M., Chisaka, O., Manley, N.R., Capecchi, M.R., 1993. Loss of Hox-A1 (Hox-1.6) function results in the reorganization of the murine hindbrain. Development 118, 1063–1075.

Chandrasekhar, A., Moens, C.B., Warren Jr., J.T., Kimmel, C.B., Kuwada, J.Y., 1997. Development of branchiomotor neurons in zebrafish. Development 124, 2633–2644.

Chen, H., Namkung, M.J., Juchau, M.R., 1995. Biotransformation of all-trans-retinol and all-trans-retinal to all-trans-retinoic acid in rat conceptal homogenates. Biochem. Pharmacol. 50, 1257–1264.

Connor, M.J., Smit, M.H., 1987. Terminal-group oxidation of retinol by mouse epidermis. Inhibition in vitro and in vivo. Biochem. J. 244, 489–492.

Dickman, E.D., Thaller, C., Smith, S.M., 1997. Temporally-regulated retinoic acid depletion produces specific neural crest, ocular and nervous system defects. Development 124, 3111–3121.

Dupé, V., Lumsden, A., 2001. Hindbrain patterning involves graded responses to retinoic acid signalling. Development 128, 2199–2208.

Dupé, V., Ghyselinck, N.B., Wendling, O., Chambon, P., Mark, M., 1999. Key roles of retinoic acid receptors alpha and beta in the patterning of the caudal hindbrain, pharyngeal arches and otocyst in the mouse. Development 126, 5051–5059.

Durston, A.J., Timmermans, J.P., Hage, W.J., Hendriks, H.F., de Vries, N.J., Heideveld, M., Nieuwkoop, P.D., 1989. Retinoic acid causes an anteroposterior transformation in the developing central nervous system. Nature 340, 140–144.

Eichele, G., 1997. Retinoids: from hindbrain patterning to Parkinson disease. Trends Genet. 13, 343–345.

Fritzsch, B., 1996. Development of the labyrinthine efferent system. Ann. N. Y. Acad. Sci. 781, 21–33.

Gale, E., Zile, M., Maden, M., 1999. Hindbrain respecification in the retinoid-deficient quail. Mech. Dev. 89, 43–54.

Gavalas, A., Krumlauf, R., 2000. Retinoid signalling and hindbrain patterning. Curr. Opin. Genet. Dev. 10, 380–386.

Germain, P., Iyer, J., Zechel, C., Gronemeyer, H., 2002. Co-regulator recruitment and the mechanism of retinoic acid receptor synergy. Nature 415, 187–192.

Gilland, E., Baker, R., 1993. Conservation of neuroepithelial and mesodermal segments in the embryonic vertebrate head. Acta Anat. (Basel) 148, 110–123.

Goddard, J.M., Rossel, M., Manley, N.R., Capecchi, M.R., 1996. Mice with targeted disruption of Hoxb-1 fail to form the motor nucleus of the VIIth nerve. Development 122, 3217–3228.

Grandel, H., Lun, K., Rauch, G.J., Rhinn, M., Piotrowski, T., Houart, C., Sordino, P., Kuchler, A.M., Schulte-Merker, S., Geisler, R., Holder, N., Wilson, S.W., Brand, M., 2002. Retinoic acid signalling in the zebrafish embryo is necessary during pre-segmentation stages to pattern the an-

terior–posterior axis of the CNS and to induce a pectoral fin bud. Development 129, 2851–2865.

Higashijima, S., Hotta, Y., Okamoto, H., 2000. Visualization of cranial motor neurons in live transgenic zebrafish expressing green fluorescent protein under the control of the islet-1 promoter/enhancer. J. Neurosci. 20, 206–218.

Hill, J., Clarke, J.D., Vargesson, N., Jowett, T., Holder, N., 1995. Exogenous retinoic acid causes specific alterations in the development of the midbrain and hindbrain of the zebrafish embryo including positional respecification of the Mauthner neuron. Mech. Dev. 50, 3–16.

Holder, N., Hill, J., 1991. Retinoic acid modifies development of the midbrain–hindbrain border and affects cranial ganglion formation in zebrafish embryos. Development 113, 1159–1170.

Inoue, A., Takahashi, M., Hatta, K., Hotta, Y., Okamoto, H., 1994. Developmental regulation of islet-1 mRNA expression during neuronal differentiation in embryonic zebrafish. Dev. Dyn. 199, 1–11.

Kikonyogo, A., Abriola, D.P., Dryjanski, M., Pietruszko, R., 1999. Mechanism of inhibition of aldehyde dehydrogenase by citral, a retinoid antagonist. Eur. J. Biochem. 262, 704–712.

Kimmel, C.B., Ballard, W.W., Kimmel, S.R., Ullmann, B., Schilling, T.F., 1995. Stages of embryonic development of the zebrafish. Dev. Dyn. 203, 253–310.

Krauss, S., Maden, M., Holder, N., Wilson, S.W., 1992. Zebrafish pax[b] is involved in the formation of the midbrain–hindbrain boundary. Nature 360, 87–89.

Lang, D.M., Warren Jr., J.T., Klisa, C., Stuermer, C.A., 2001. Topographic restriction of TAG-1 expression in the developing retinotectal pathway and target dependent reexpression during axon regeneration. Mol. Cell. Neurosci. 17, 398–414.

Maden, M., 2002. Retinoid signalling in the development of the central nervous system. Nat. Rev., Neurosci. 3, 843–853.

Maden, M., Gale, E., Kostetskii, I., Zile, M., 1996. Vitamin A-deficient quail embryos have half a hindbrain and other neural defects. Curr. Biol. 6, 417–426.

Marx, M., Rutishauser, U., Bastmeyer, M., 2001. Dual function of polysialic acid during zebrafish central nervous system development. Development 128, 4949–4958.

Mic, F.A., Haselbeck, R.J., Cuenca, A.E., Duester, G., 2002. Novel retinoic acid generating activities in the neural tube and heart identified by conditional rescue of Raldh2 null mutant mice. Development 129, 2271–2282.

Moens, C.B., Cordes, S.P., Giorgianni, M.W., Barsh, G.S., Kimmel, C.B., 1998. Equivalence in the genetic control of hindbrain segmentation in fish and mouse. Development 125, 381–391.

Morriss-Kay, G.M., Sokolova, N., 1996. Embryonic development and pattern formation. FASEB J. 10, 961–968.

Morriss-Kay, G.M., Ward, S.J., 1999. Retinoids and mammalian development. Int. Rev. Cytol. 188, 73–131.

Niederreither, K., McCaffery, P., Dräger, U.C., Chambon, P., Dolle, P., 1997. Restricted expression and retinoic acid-induced downregulation of the retinaldehyde dehydrogenase type 2 (RALDH-2) gene during mouse development. Mech. Dev. 62, 67–78.

Niederreither, K., Subbarayan, V., Dolle, P., Chambon, P., 1999. Embryonic retinoic acid synthesis is essential for early mouse post-implantation development. Nat. Genet. 21, 444–448.

Niederreither, K., Vermot, J., Schuhbaur, B., Chambon, P., Dolle, P., 2000. Retinoic acid synthesis and hindbrain patterning in the mouse embryo. Development 127, 75–85.

Niederreither, K., Vermot, J., Fraulob, V., Chambon, P., Dolle, P., 2002. Retinaldehyde dehydrogenase 2 (RALDH2)-independent patterns of retinoic acid synthesis in the mouse embryo. Proc. Natl. Acad. Sci. U. S. A. 99, 16111–16116.

Ott, H., Diekmann, H., Stuermer, C.A., Bastmeyer, M., 2001. Function of Neurolin (DM-GRASP/SC-1) in guidance of motor axons during zebrafish development. Dev. Biol. 235, 86–97.

Oxtoby, E., Jowett, T., 1993. Cloning of the zebrafish krox-20 gene (krx-20) and its expression during hindbrain development. Nucleic Acids Res. 21, 1087–1095.

Perz-Edwards, A., Hardison, N.L., Linney, E., 2001. Retinoic acid-mediated gene expression in transgenic reporter zebrafish. Dev. Biol. 229, 89–101.

Prince, V.E., Moens, C.B., Kimmel, C.B., Ho, R.K., 1998. Zebrafish hox genes: expression in the hindbrain region of wild-type and mutants of the segmentation gene, valentino. Development 125, 393–406.

Russo, J.E., Hauguitz, D., Hilton, J., 1988. Inhibition of mouse cytosolic aldehyde dehydrogenase by 4-(diethylamino)benzaldehyde. Biochem. Pharmacol. 37, 1639–1642.

Russo, J., Barnes, A., Berger, K., Desgrosellier, J., Henderson, J., Kanters, A., 2002. 4-(*N*,*N*-dipropylamino)benzaldehyde inhibits the oxidation of all-trans retinal to all-trans retinoic acid by ALDH1A1, but not the differentiation of HL-60 promyelocytic leukemia cells exposed to all-trans retinal. BMC Pharmacol. 2, 4.

Studer, M., Lumsden, A., Ariza-McNaughton, L., Bradley, A., Krumlauf, R., 1996. Altered segmental identity and abnormal migration of motor neurons in mice lacking Hoxb-1. Nature 384, 630–634.

Vallari, R.C., Pietruszko, R., 1982. Human aldehyde dehydrogenase: mechanism of inhibition of disulfiram. Science 216, 637–639.

van der Wees, J., Schilthuis, J.G., Koster, C.H., Diesveld-Schipper, H., Folkers, G.E., van der Saag, P.T., Dawson, M.I., Shudo, K., van der Burg, B., Durston, A.J., 1998. Inhibition of retinoic acid receptor-mediated signalling alters positional identity in the developing hindbrain. Development 125, 545–556.

Veverka, K.A., Johnson, K.L., Mays, D.C., Lipsky, J.J., Naylor, S., 1997. Inhibition of aldehyde dehydrogenase by disulfiram and its metabolite methyl diethylthiocarbamoyl-sulfoxide. Biochem. Pharmacol. 53, 511–518.

Weiland, U.M., Ott, H., Bastmeyer, M., Schaden, H., Giordano, S., Stuermer, C.A., 1997. Expression of an L1-related cell adhesion molecule on developing CNS fiber tracts in zebrafish and its functional contribution to axon fasciculation. Mol. Cell. Neurosci. 9, 77–89.

Wendling, O., Dennefeld, C., Chambon, P., Mark, M., 2000. Retinoid signaling is essential for patterning the endoderm of the third and fourth pharyngeal arches. Development 127, 1553–1562.

Wendling, O., Ghyselinck, N.B., Chambon, P., Mark, M., 2001. Roles of retinoic acid receptors in early embryonic morphogenesis and hindbrain patterning. Development 128, 2031–2038.

Westerfield, M., 1995. The Zebrafish Book. Guide for the Laboratory Use of Zebrafish (Danio rerio). Univ. of Oregon Press, Eugene.

White, J.C., Highland, M., Kaiser, M., Clagett-Dame, M., 2000. Vitamin A deficiency results in the dose-dependent acquisition of anterior character and shortening of the caudal hindbrain of the rat embryo. Dev. Biol. 220, 263–284.